Prognostics in Battery Health Management

Kai Goebel, Bhaskar Saha, Abhinav Saxena, Jose R. Celaya, and Jon P. Christophersen

Source: NASA collection. http://www.jpl.nasa.gov/history/90s/Mars_Global Surveyor_1997.htm

Prognostics and Health Management (PHM) has had a recent resurgence for two reasons new service offerings for industry that guarantee uptime and because military requirements are including cost-containing condition-based maintenance implementations. Although a chief component of PHM is prognostics, it is also its least mature element. Prognostics attempts to estimate remaining component life when an abnormal condition has been detected. The key to useful prognostics is not only an accurate remaining life estimate, but also an assessment of the confidence of the uncertainty estimate. The latter is often expressed through a probability density function (pdf) that allows the computation of confidence bounds. It is the uncertainty estimate that poses particular challenges to the prediction of remaining component life, since it must account for data from measurements, state estimation, model inaccuracies, future load uncertainty, etc.

Batteries are a core component of many machines and are critical to the system's functional capabilities. Battery failure could lead to reduced performance, operational impairment, and even catastrophic failure, especially in aerospace systems. An efficient method for battery monitoring would greatly improve the reliability of such systems.

The phrase "battery health monitoring" has a wide variety of connotations, ranging from intermittent manual measurements of voltage and electrolyte specific gravity to fully automated online supervision of various measured and estimated battery parameters. In the aerospace application domain, researchers have looked at the various failure modes of the battery subsystems. An aerospace catastrophic battery failure occurred in NASA's Mars Global Surveyor, which stopped operating in November 2006. Preliminary investigations revealed that the spacecraft was commanded to go into a safe mode, which positioned the radiator for the batteries toward the sun. This increased the temperature of the batteries, and they lost their charge capacity. This failure is not the only one of its kind in aerospace applications.

Different battery diagnostic methods have been evaluated for aerospace applications, like discharge to a fixed cut-off voltage, open circuit voltage, voltage under load, electrochemical impedance spectrometry (EIS) [1], and combining conductance technology with other measured parameters like battery temperature/differential information and the amount of float charge [2]. An efficient method of PHM for batteries would greatly improve the reliability of these systems.

In applications for use in hybrid electric and plug-in hybrid electric vehicles, PHM dynamic models have been built for lithium ion batteries. These models take into consideration nonlinear equilibrium potentials, rate and temperature dependencies, thermal effects, and transient power response [3]. Sophisticated reasoning schemes have been applied to feature vectors with the goal of estimating state-of-charge (SOC), state-of-health (SOH), and state-of-life (SOL). However, it still remains difficult to accurately predict the end-of-life of a battery from estimates of SOC and SOH when environmental and load conditions differ from the training data set.

In this article, we examine PHM issues using battery health management of Gen 2 cells, an 18650-size lithium-ion cell, as

1094-6969/08/$25.00©2008IEEE

Table 1 – Li-ion Cell (ATD Gen 2 Cell Baseline) Chemistry	
Positive Electrode	8 wt% PVDF binder
	4 wt% SFG-6 graphite
	4 wt% carbon black
	84 wt% $LiNi_{0.8}Co_{0.15}Al_{0.05}O_2$
Negative Electrode	8 wt% PVDF binder
	92 wt% MAG-10 graphite
Electrolyte	1.2 M $LiPF_6$ in EC:EMC (3:7 wt%)
Separator	25 µm thick PE (Celgard)

a test case. We will show where advanced regression, classification, and state estimation algorithms have an important role in the solution of the problem and in the data collection scheme for battery health management that we used for this case study [4].

Data from Lithium-ion Cells

Life-cycle test data have been collected from second generation, Gen 2, 18650-size lithium-ion cells at the Idaho National Laboratory (INL) under the Advanced Technology Development (ATD) Program. This program was initiated in 1998 by the U.S. Department of Energy, Office of Vehicle Technologies to find solutions to the barriers that limit the commercialization of high-power lithium-ion batteries for hybrid electric and plug-in hybrid electric vehicles. The barriers limiting these batteries are poor low-temperature performance, abuse tolerance, and accurate life prediction. Many other researchers in electric and hybrid vehicles have also focused on battery health monitoring [5].

Cells were aged at various temperatures, states of charge, and other stress conditions to establish behavior. Performance tests were used to establish changes in the baseline. The Gen 2 cell testing involved exhaustive evaluation of baseline and variant cells and was distributed among three national laboratories with a test matrix consisting of three SOCs (60, 80, and 100%), four temperatures (25, 35, 45, and 55°C), and three life tests (calendar-life, cycle-life, and accelerated-life) [6]. Completion of all the tests took four years.

The data used in our study were from cells that were cycle-life tested at 60% SOC and temperatures (25°C and 45°C). Table 1 gives the chemical details of the cells under test.

As part of the reference performance test for these Gen 2 cells, EIS measurements were made periodically to determine impedance changes in the electrode–electrolyte interface as a function of cell life. EIS measurements were initiated by discharging the cells from a fully-charged state to the specified open circuit voltage (OCV) corresponding to the target SOC. Changes in the internal parameters of the battery are observed as shifts in EIS data plots and characterize battery capacity degradation. Following an eight to twelve-hour rest at OCV, which allowed the cells to reach electrochemical equilibrium, the impedance was measured using a four-terminal connection over a frequency range of 10 kHz to 0.01 Hz, with

Fig. 1. (a) Thermal block with cells (INL) (b) Prognostic test bed at NASA ARC.

a minimum of eight points per decade of frequency. This test was performed on all cells at 60% SOC.

All testing was performed with cells placed in environmental chambers to control ambient temperature. The chambers control the temperature to within ±3°C, as specified in the test plan [6]. Also, all Gen 2 cells were placed in

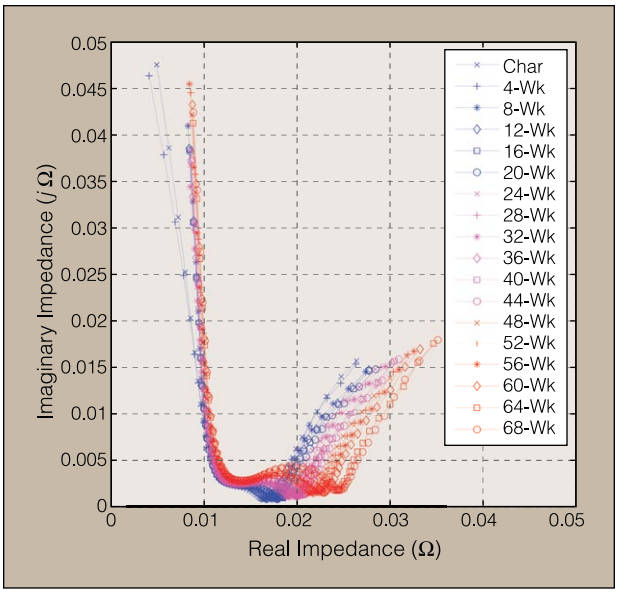

Fig. 2. This graph shows the shift in EIS impedance data from a Gen 2 cell with ageing at 25°C and 60% SOC.

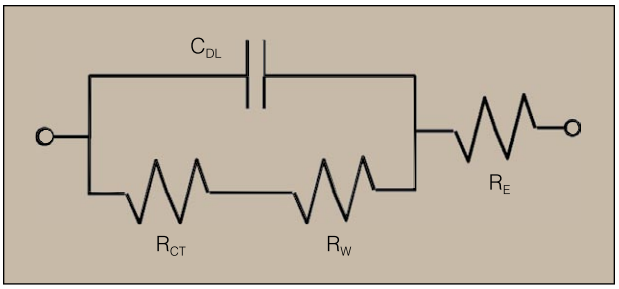

Fig. 3. A Lumped-Parameter Model of a Lithium-ion Cell.

thermal blocks to more uniformly control the cell temperature and minimize temperature transients [see Figure 1(a)]. Thermocouples were also placed on each cell to monitor temperatures during life testing. Figure 1(b) shows a similar aging setup at the NASA Ames Research Center (ARC), which will be used to further investigate different prognostic methodologies.

The cycle-life test consisted of constant power discharge and regeneration pulses with interspersed rest periods for a total duration of 72 s and was repeated continuously while centered around 60% SOC. This profile assumed a full size battery pack and must be scaled to use for a cell-size level [6]. It has been demonstrated that battery capacity degradation can be characterized through changes in the internal parameters of the battery, and these changes can be observed as shifts in EIS data plots. Figure 2 shows the shift in EIS data of a representative Gen 2 cell that was cycle-life aged at 25°C and 60% SOC.

To describe the internal parameters, the battery operation is expressed in structural and functional models, which aid in the construction of the "physics of failure mechanisms" model. Features extracted from sensor data of voltage, current, power, impedance, frequency, and temperature readings are used to estimate the internal parameters in the lumped-parameter battery model shown in Figure 3. The parameters of interest are the double layer capacitance C_{DL}, the charge transfer resistance R_{CT}, the Warburg impedance R_W, and the electrolyte resistance R_E. The values of these internal parameters change with various aging and fault processes like plate sulfation, passivation, and corrosion.

Data Processing

The values of the internal parameters define the shape and position of EIS plots and can be extracted from these plots as diagnostic features. Figure 4 shows a section of the data shown in Figure 2 with the battery internal model parameters identified. Since the Nyquist plot of a capacitance and resistance in parallel (C_{DL} and R_{CT} as shown in Figure 3) is expected to be a semicircle, we used data from the EIS curves in an automated fashion to fit semicircles to the middle portion of the graph. The fitting was performed in the least square sense as shown below:

$$\min\left\{\sum_i \left(Z_{i,\mathrm{Im}}^2 + \left(Z_{i,\mathrm{Re}} - c\right)^2 - r^2\right)^2\right\}, \qquad (1)$$

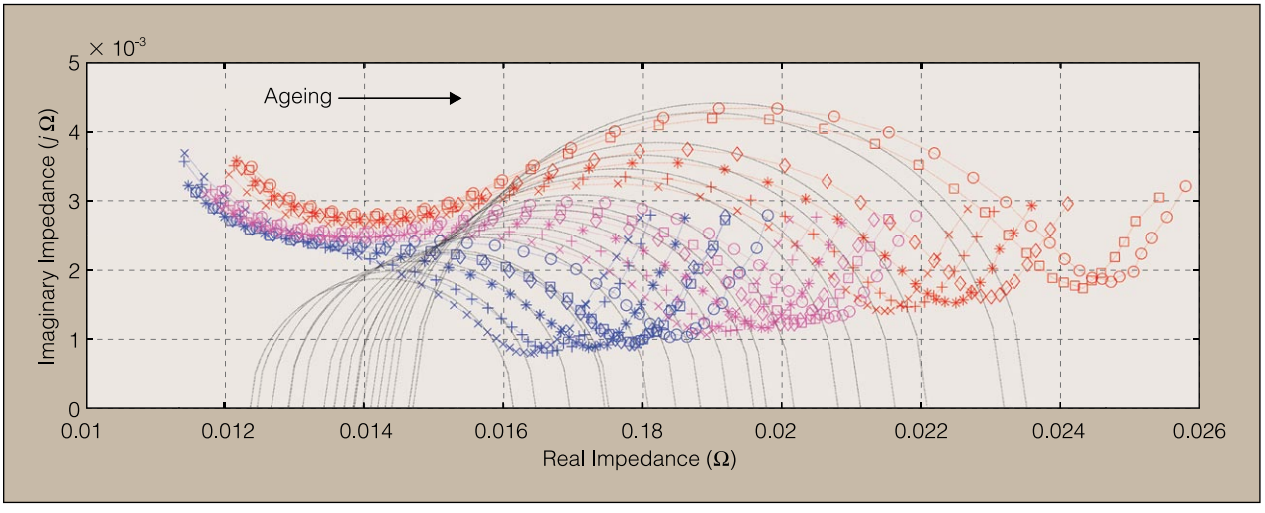

Fig. 4. Zoom in EIS Plots (60% SOC) with Internal Battery Model Parameter Identification.

where, $Z_{i,\mathrm{Im}}$ and $Z_{i,\mathrm{Re}}$ are the imaginary and real parts of impedance of data point *i* in the EIS plots of Figure 4. The center, c, is (on the x-axis) and the radius of the fitted semicircle is *r*. The left intercept of the semicircles gives the R_E values while the diameters of the semicircles give the R_{CT} values. Other internal parameters showed negligible change over the aging process and are hence ignored for further analysis.

We noted that there was a very high degree of linear correlation between the C/1 capacity (capacity at nominal rated current of 1A) and the internal impedance parameter R_E+R_{CT} (Figure 5). We will show how this relationship can be exploited to estimate the current and future C/1 capacities.

METHODS

The main objective of this study was to develop prognostics algorithms to predict remaining life of the batteries with high confidence. We also wanted to compare various prediction techniques for their strengths and weaknesses in addressing the issues of accuracy of predictions and uncertainty management against various trade-offs, like complexity and computational burden, which may be crucial for some real-time applications. Starting with very simple statistical regression techniques, we applied more sophisticated probabilistic regression and advanced state estimation based hybrid algorithms to cover a wide range of algorithms. These techniques and corresponding results are presented next.

Statistics Based Baseline Model

We first employed a simple data-driven routine to establish a baseline for battery health prediction performance and uncertainty assessment. We then employed more sophisticated models to improve on this baseline. Battery health is directly tied to capacity. The battery is considered to be in a failed state when its capacity has faded by 30%. We constrained the problem by making available only information from batteries aged under specific environmental conditions to then predict the end-of-life of batteries operating under different environmental conditions (and therefore aging at different, unknown rates). EIS measurements were provided as health monitoring data to help with the state assessment. Performance assessment was done at specified intervals by measuring the accuracy of prediction. In addition, an uncertainty assessment was carried out to qualify the goodness of the prediction. For the data-driven approach, one can glean, from the relationship between R_E+R_{CT} and the capacity C/1 at baseline temperature (25°C), the equivalent damage threshold in the R_E+R_{CT}, i.e., d_{th}=0.033.

We also explored more sophisticated robust linear regression techniques like robust minimum m (MM)-regression and the robust-LTS (Least Trimmed sum of Squares) regression to extract this relationship. These methods are resistant to outliers and robust to deviations from a Gaussian distribution. The results are similar to those obtained from the simpler method discussed above and ratify the damage threshold d_{th}=0.033. Next, via extracted features from the EIS measurements, R_E+R_{CT} can be tracked at elevated temperatures (here, 45°C). Ignoring the first two data points (which behave similar to what is considered as "wear-in" pattern in other domains), a second degree polynomial is used at the prediction points to extrapolate out to the damage threshold. Confidence bounds are projected to

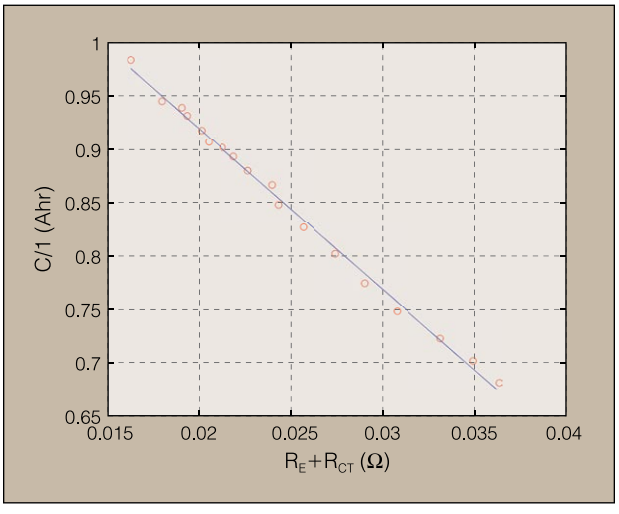

Fig. 5. Linear correlation between capacity, C/1, and impedance parameters, R_E +R_{CT}.

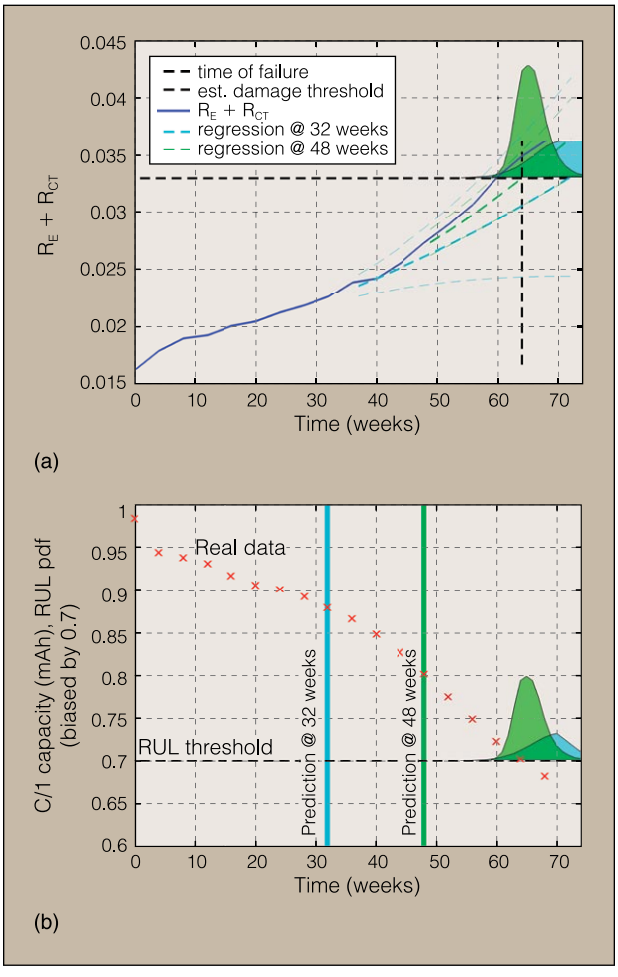

Fig. 6. Extrapolation to damage threshold and resulting uncertainty distribution; (a) Regression on R_E+R_{CT} (b) Capacity predictions obtained by superimposing predicted R_E +R_{CT} into capacity-time domain.

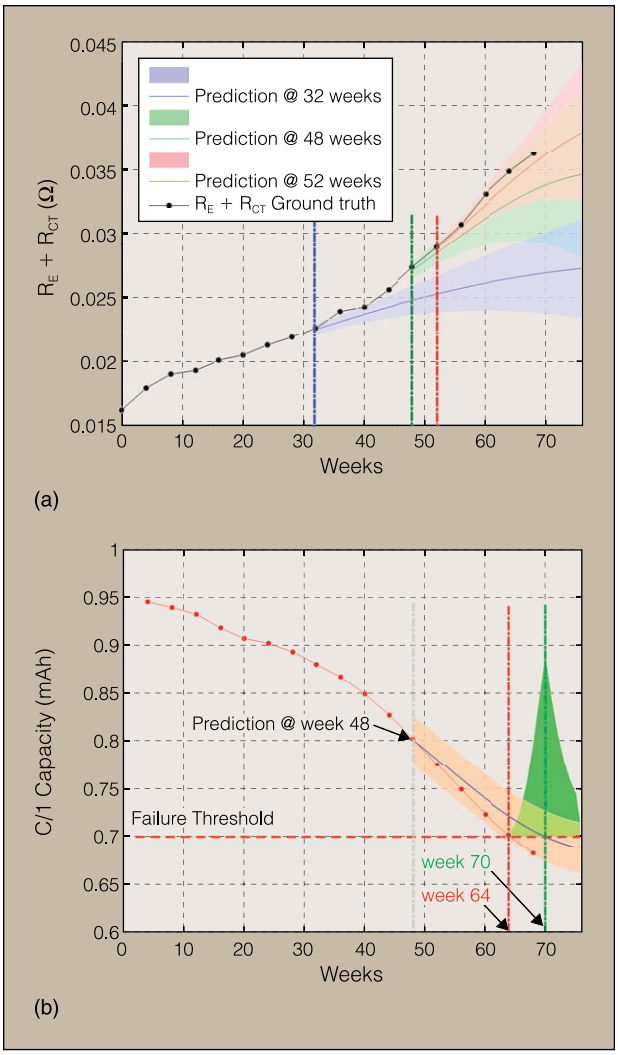

Fig. 7. (a). $R_E + R_{CT}$ predictions (with 95% confidence bounds) using GPR at weeks 32, 48, and 52 (b). End-of-life predictions (with 95% confidence bounds) for battery capacity using GPR at week 48.

the damage threshold to show the uncertainty distribution around the prediction. Figure 6(a) illustrates that the prediction accuracy at prediction point t=32 weeks is rather poor. The prediction is late by 7.55 weeks and the associated uncertainty has extremely wide tails, particularly on the right side.

In contrast, prediction accuracy performed at t=48 weeks is almost perfect, with an error of only 0.01 weeks. The resulting uncertainty distribution is much narrower, although it is still somewhat large on the right. Therefore, we establish that simpler methods can yield a fairly good estimate in situations like these. However, the confidence in these predictions is rather low and may not be favorable in critical applications. Note that in the example shown in Figure 6(b), the time when capacity has faded by 30% (at time t=64) does not agree completely with the time at which d_{th}=0.033 (t=59). This reflects that the R_E+R_{CT} model is not a very good model for damage propagation after all.

Probabilistic Regression Model

We then explored a Gaussian Process Regression (GPR) method to estimate the end-of-life. GPR is a probabilistic technique for nonlinear regression that computes posterior degradation estimates by constraining the prior distribution to fit the available training data [7]. It provides variance around its mean predictions to describe associated uncertainty in the predictions. We used GPR to regress the evolution of internal parameters (R_E+R_{CT}) of the battery with time at 45°C. The relationship between these parameters and the battery capacity was again learned from experimental data at 25°C. As stated earlier, battery capacity was linearly related to the internal parameter values, and when regressed through GPR, almost constant confidence bounds were obtained for this relationship. We regressed the internal parameters with time and transferred the predicted values to the capacity domain to express capacity decay with time.

We observed that GPR, being a probabilistic approach, fails to learn internal parameter evolution with only a few training data points when exposed to data up to only t=32 weeks. Figure 7(a) shows three predictions (at 32, 48, and 52 weeks) for the evolution of R_E+R_{CT} with time. A 95% confidence bound has been included in the plots. Increasing width of these bounds represents low confidence in prediction points where no learning data were available. It should be noted that only the mean values from the R_E+R_{CT} evolution curve [Figure 7(a)] were used to predict the capacity. This prediction was based on capacity versus time mapping and thus inherited its almost constant confidence bounds. As shown in Figure 7(a) since the prediction at t=32 weeks fails to follow the actual trend, it leads to extremely late end-of-life predictions. However, with some more learning data up to t=48 weeks it picks up the trend fairly well. Corresponding end-of-life pdf is shown in Figure 7(b). The end-of-life prediction at t=48 weeks is 70 weeks with an error of +6 weeks of late prediction. These predictions got more accurate and precise as more data were made available for learning. Therefore, we conclude that although more sophisticated approaches like GPR are helpful in characterizing the uncertainty in the predictions, they need sufficient statistical data to properly learn the nonlinear dynamics of the process.

Particle Filter Model

The behavior of the previous methods indicates that the regression techniques fail to learn non-linear trends in the absence of full-range training data. For such situations, one must be able to track trends as they change and modify predictions to conform to established degradation models. With this goal in mind, we then examined particle filters: the state of the art in prediction technology. Particles filters not only use the information available from the process measurements but also incorporate any models available for the process. This technique also has the ability to tune non-stationary model parameters simultaneously with state estimation, which combined with the representation of state space as multiple weighted particles, makes it ideal for state tracking and prediction.

In this application, we combine them with Relevance Vector Machines (RVMs). The RVM is a form of machine learning that uses Bayesian inference to obtain sparse solutions for regression and classification. In RVM regression, the task is to probabilistically learn the nonlinear patterns in data, which is

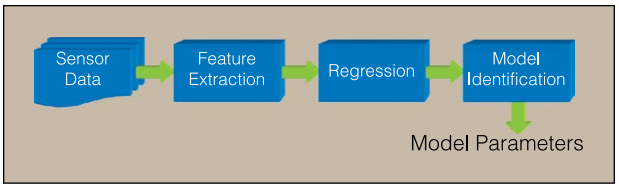

Fig. 8. Schematic of Decay Model Development.

multidimensional (say n_{dim}), using an n_{dim}-1 dimensional *hyperplane* in kernel-transformed *hyperspace* where the problem becomes linear [8]. The overall process is broken down into an offline (learning) and an online (tracking and prediction) part. During offline analysis, relevance vector machine regression is performed to find representative aging curves. Exponential growth models, as shown in equation 2, are then fitted on these curves to identify the relevant decay parameters like C and λ:

$$\theta = C\exp(-\lambda t), \tag{2}$$

where θ is a internal battery model parameter like R_{CT} or R_E. The overall model development scheme is depicted in the flowchart of Figure 8.

Particle Filters Background

Bayesian techniques provide a general rigorous framework for dynamic state estimation problems. The core idea is to construct a pdf of the state based on all available information. For a linear system with Gaussian noise, the method reduces to the Kalman filter. The state space pdf remains Gaussian at every iteration, and the filter equations propagate and update the mean and covariance of the distribution. For nonlinear systems or non-Gaussian noise, there is no general analytic (closed form) solution for the state space pdf. The most popular solution to the recursive nonlinear state estimation problem is the extended Kalman filter (EKF). In that approach, the estimation problem is linearized about the predicted state so that the Kalman filter can be applied. The desired pdf is approximated by a Gaussian, which may have significant deviation from the true distribution causing the filter to diverge.

In contrast, for the *Particle Filter* (PF) approach [9], the pdf is approximated by a set of particles (points) representing sampled values from the unknown state space and a set of associated weights denoting discrete probability masses. The particles are generated and recursively updated from a nonlinear process model that describes the evolution in time of the system under analysis, a measurement model, a set of available measurements, and an a *priori* estimate of the state pdf. In other words, PF is a technique for implementing a recursive Bayesian filter using Monte Carlo (MC) simulations and is known as a sequential MC (SMC) method.

Implementation

The state and measurement equations that describe the battery model are given below:

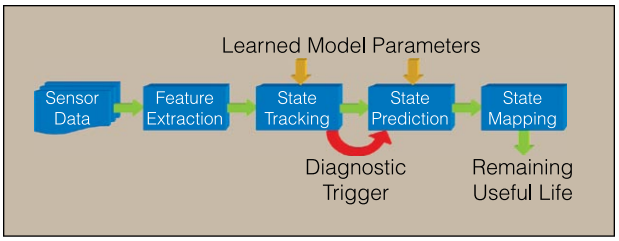

Fig. 9. Particle Filter Framework.

$$\begin{aligned} z_0 &= C\,;\Lambda_0 = \Lambda \\ z_k &= z_{k-1}\ \exp(-\Lambda_k) + \omega_k \\ \Lambda_k &= \Lambda_{k-1} + \nu_k \\ x_k &= [z_k\,;\Lambda_k] \\ y_k &= z_k + \upsilon_k \end{aligned} \tag{3}$$

where the vector z is comprised of R_E and R_{CT}, and the matrices C and Λ contain their decay parameters C and λ values, respectively. The z and Λ vectors are combined to form the state vector x. The measurement vector y is comprised of the battery parameters inferred from measured data. The time index is denoted by k. The values of the C and Λ vectors (for both R_E and R_{CT}) learned from RVM regression are used to initialize the particle filter. The noise samples ω, ν, and υ are picked from zero mean Gaussian distributions whose standard deviations are derived from the given training data, thus accommodating for the sources of uncertainty in feature extraction, regression modeling, and measurement. System importance resampling of the particles is carried out in each iteration to reduce the degeneracy of particle weights. This helps in maintaining the track of the state vector even under the presence of disruptive effects like unmodeled operational conditions (in our case, high temperatures).

The system description model developed in the offline process is fed into the online process where the particle filtering prognosis framework is triggered by a diagnostic routine. The algorithm incorporates the model parameter as an additional component of the state vector and performs parameter identification in parallel with state estimation. Predicted values of the internal battery model parameters are used to calculate expected charge capacities of the battery. The current capacity estimate is used to compute the SOC while the future predictions are compared against end-of-life thresholds to derive remaining useful life (RUL) estimates. Figure 9 shows a simplified schematic of the process described above.

For the test data, the estimated λ value for the R_{CT} growth model (equation 2) is considerably larger than of the training data (collected at 25°C), i.e., λ_{test}=0.1123 compared to λ_{train}=0.0125. RUL is derived by extrapolating out the capacity estimates (of the 100 particles used in this application) into the future (Figure 10) until predicted capacity hits a certain predetermined end-of-life threshold. The weight vector of the PF algorithm is used to calculate the RUL distribution.

The particle filter approach yields an RUL error of 5.8545 weeks early, at week 32, and an error of 2.59 weeks early for predictions made at week 48. In comparison to the other approaches that have been discussed, the PF results are more accurate. More

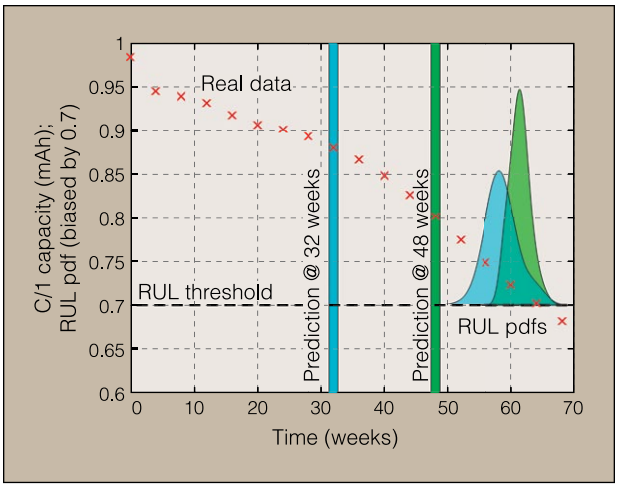

Fig. 10. Capacity prediction using particle filter.

importantly, early predictions are considered more favorable than late predictions to avoid any unanticipated failures provided, of course, that the error is reasonable. In terms of error bounds, it simply means that the acceptable limit is wider for early predictions than for those that are late. The results also show that the RUL pdf improves in both accuracy (closeness of the mean to the actual RUL) and precision (narrowness of the pdf, indicating higher confidence in the mean value) as more measurements are included. This indicates that Bayesian statistical approaches are well suited to handle various sources of uncertainties since they define probability distributions over both parameters and variables and integrate out the nuisance terms.

Conclusion

Batteries represent complex systems whose internal state variables are either inaccessible to sensors or hard to measure under operational conditions. This work exemplifies how more detailed model information and more sophisticated prediction techniques can improve both the accuracy as well as the residual uncertainty of the prediction in Prognostics and Health Management. The more dramatic performance improvement between various prediction techniques is in their ability to learn complex non-linear degradation behavior from the training data and discard any external noise disturbances.

An algorithm that manages these sources of uncertainty well can yield higher confidence in predictions, expressed by narrower uncertainty bounds. We observed that the particle filter approach results in RUL distributions which have better precision (narrower pdfs) by several σs (if approximated as Gaussian) as compared to the other regression methods. However, PF requires a more complex implementation and computational overhead than the other methods. This illustrates the basic tradeoff between modeling and algorithm development versus prediction accuracy and precision. For situations like battery health management where the rate of capacity degradation is rather slow, one can rely on simple regression methods that tend to perform well as more data are accumulated and still predict far enough in advance to avoid any catastrophic failures. Techniques like GPR or even the baseline approach can offer a suitable platform in these situations by managing the uncertainty fairly well with much simpler implementations. Other data sets may allow much smaller prediction horizons and hence require precise techniques like particle filters.

In this study, we conclude that there are several methods one could employ for battery health management applications. Based on end user requirements and available resources, a choice can be made between simple or more elegant techniques. The particle filter based approach emerges as the winner when accuracy and precision are considered more important than other requirements.

References

[1] D. G. Vutetakis, V. V. Viswanathan, "Determining the State-of-Health of Maintenance-Free Aircraft Batteries", *Proc. of the Tenth Annual Battery Conference on Applications and Advances 1995*, 1995, pp 13-18.

[2] D. C. Cox, R. Perez-Kite, "Battery state of health monitoring, combining conductance technology with other measurement parameters for real-time battery performance analysis", *Twenty-second International Telecommunications Energy Conference 2000*, INTELEC, pp. 342 - 347, Sep. 2000.

[3] L. Gao, S. Liu, R. A. Dougal, "Dynamic Lithium-Ion Battery Model for System Simulation", *IEEE Trans. on Components and Packaging Technologies*, vol. 25, no. 3, pp. 495-505, Sep. 2002.

[4] B. Saha, K. Goebel, S. Poll, J. Christopherson, "An Integrated Approach to Battery Health Monitoring using Bayesian Regression, Classification and State Estimation", Proceedings of AUTOTESTCON 2007, 2007.

[5] E. Meissner, G. Richter, "Battery Monitoring and Electrical Energy Management - Precondition for future vehicle electric power systems", *Journal of Power Sources*, vol. 116, no. 1, pp. 79-98(20), July 2003.

[6] PNGV Test Plan for Advanced Technology Development Gen 2 Lithium-Ion Cells, *EVH-TP-121*, Revision 6, October 2001.

[7] C. E. Rasmussen, and C. K. I. Williams, *Gaussian Processes for Machine Learning*, The MIT Press Cambridge MA, 2006.

[8] M. E. Tipping, "The Relevance Vector Machine", *Advances in Neural Information Processing Systems*, Cambridge MIT Press, 2000, vol. 12, pp. 652-658

[9] N. J. Gordon, D. J. Salmond, and A. F. M. Smith, "Novel approach to nonlinear/non-Gaussian Bayesian state estimation", *IEE Proceedings F:Radar and Signal Processing*, vol. 140, no. 2, pp. 107-113, April 1993.

Kai Goebel (kai.goebel@nasa.gov) is a senior scientist at NASA Ames Research Center, where he leads the Prognostics Center of Excellence (prognostics.arc.nasa.gov). Prior to that, he worked at General Electric's Global Research Center in Niskayuna, NY, from 1997 to 2006 as a senior research scientist. He has carried out applied research in the areas

of artificial intelligence, soft computing, and information fusion. His research interest lies in advancing these techniques for real time monitoring, diagnostics, and prognostics. He has fielded numerous applications for aircraft engines, transportation systems, medical systems, and manufacturing systems. He holds half a dozen patents and has published more than 75 papers. He received the degree of Diplom-Ingenieur from the Technische Universität München, Germany, in 1990, and the M.S. and Ph.D. from the University of California at Berkeley in 1993 and 1996, respectively.

Bhaskar Saha is a Research Programmer with Mission Critical Technologies at the Prognostics Center of Excellence, NASA Ames Research Center. His research is focused on applying various classification, regression, and state estimation techniques for predicting remaining useful life of systems and their components. He has also published a fair number of papers on these topics. Bhaskar completed his Ph.D. from the School of Electrical and Computer Engineering at Georgia Institute of Technology in 2008. He received his M.S. from the same school and his B. Tech. (Bachelor of Technology) degree from the Department of Electrical Engineering, Indian Institute of Technology, Kharagpur.

Abhinav Saxena is a Staff Scientist with Research Institute for Advanced Computer Science at the Prognostics Center of Excellence, NASA Ames Research Center. His research focus lies in developing prognostic algorithms for engineering systems. He has a Ph.D. in Electrical and Computer Engineering from Georgia Institute of Technology, Atlanta. He earned his B.Tech in 2001 from Indian Institute of Technology (IIT) Delhi, and Masters Degree in 2003 from Georgia Tech. Abhinav has been a GM manufacturing scholar and also a member of Eta Kappa Nu and Gamma Beta Phi engineering honor societies, along with IEEE and ASME.

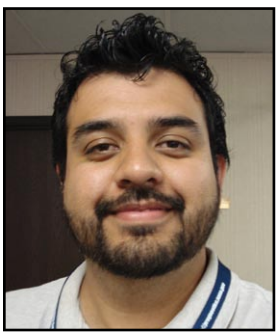

Jose R. Celaya is a visiting scientist with Research Institute for Advanced Computer Science at the Prognostics Center of Excellence, NASA Ames Research Center. He is a Ph.D. candidate in Decision Science and Engineering Systems from Rensselaer Polytechnic Institute, from where he obtained a Master of Science degree in Electrical Engineering in 2003, and has a B.S. in Cybernetics Engineering from CETYS University in 2001.

Jon P. Christophersen is a research engineer with the Energy Storage and Transportation Systems Department at the Idaho National Laboratory in Idaho Falls, ID. He has lead responsibility for all high power cell testing, analyses, and reporting under the Advanced Technology Development Program, as well as various FreedomCAR deliverables. This includes the investigation and successful implementation of novel testing profiles and procedures, developing new analysis techniques, developing and validating various life predictive modeling tools, and coordinating complex testing and analyses between various national laboratories. He has over 20 publications and numerous conference presentations related to energy storage. Mr. Christophersen received a B.S. and M.S. in electrical engineering from the University of Idaho in Moscow, ID in 1999 and 2005, respectively.